Interactive Cutting Method for Physics-based Electrosurgery Simulation

Yoshihiro Kuroda* Osaka University
Shota Tanaka† Osaka University
Masataka Imura‡ Osaka University
Osamu Oshiro§ Osaka University

Abstract

Virtual reality-based electrosurgical simulators are demanded for training of the major skills in laparoscopic surgery to reduce complications. However, foregoing studies have never proposed the physics-based real-time electrosurgery simulation, because of the complexity of the phenomena and computational costs. The aim of this study is to construct an interactive surgical simulator with a unified physics-based modeling of whole processes of electrosurgery. In this paper, we proposed an interactive simulation method of physics-based electrosurgical cutting. Especially, pre-processing independent of contact information enabled simulation with user's interactive manipulation by reducing real-time calculation. The results of simulation showed that the combination of the proposed method and parallelization reduced calculation time for electric potential in the real-time process by 59.7%. The proposed method enabled interactive electrosurgical cutting with a unified physics-based modeling of whole processes of electrosurgery.

Keywords: virtual reality, medical information systems, finite element methods.

Index Terms: I.6.3 [Simulation and Modeling]: Applications; C.3 [Special-purpose and Application-based Systems]: Real-time and embedded systems—

1 Introduction

The recent progress of computer technologies has enabled an interactive physics simulator that responds to a user's manipulation and displays visual and haptic information. In clinical medicine, electrosurgery is a fundamental operation, and over 90 percent of Minimally Invasive Surgeries (MIS) utilize electrosurgery [6]. Electrosurgery consists of a series of physical phases: electrical, thermal, and structural phases, to cut soft tissue, as shown in Fig. 1. However, the foregoing electrosurgery simulators ignored underlying physical phenomena, due to their complexity and required update rate (graphics:>30Hz, haptics:>300Hz). The simulator removed the material when the temperature reached 100 °C [8, 3, 4]. The interactive electrosurgical cutting simulation has not been reported on yet.

The aim of this study is to construct an interactive surgical simulator with a unified physics-based modeling of the whole processes of electrosurgery. We have already reported on the simulation models, and found the similarity of the temperature change in electrosurgical cutting between the simulation results and real porcine livers [7]. In this paper, we propose an interactive simulation method of physics-based electrosurgical cutting. In particular, pre-processing, independent of contact information, reduces real-time calculations and enables an interactive simulation.

*e-mail: ykuroda@bpe.es.osaka-u.ac.jp
†e-mail: s-tanaka@bpe.es.osaka-u.ac.jp
‡e-mail: imura@bpe.es.osaka-u.ac.jp
§e-mail: oshiro@bpe.es.osaka-u.ac.jp

The 21st International Conference on Artificial Reality and Telexistence
November 28-30, 2011, Osaka, Japan
ISSN: 1345-1278

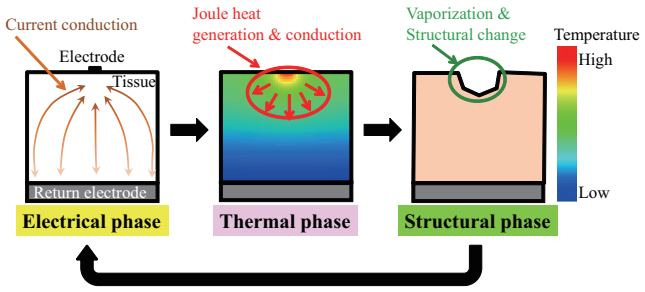

Figure 1: A series of physical phases in electrosurgery

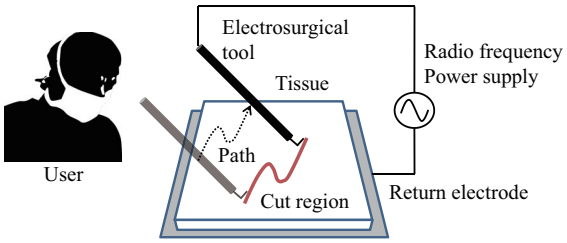

Figure 2: Electrosurgical unit

2 Physics-based Modeling of Electrosurgery

2.1 Electrosurgical unit

An electrosurgical unit is a device for cutting soft tissue by Joule heat caused by the current of high frequency, as shown in Fig. 2. The electrosurgical tool collides with tissue at a small contact area, whereas the return electrode is in contact with a large area of tissue. The electrical density around the contact area of the tool becomes high. Vaporization caused by resistive heating is thought to destruct biological tissue, although biophysical mechanisms in electrosurgery remain under investigation [2].

2.2 Electrical and thermal phases

The electrical phase determines the current density distribution caused by the contact between the electrosurgical tool and the object. The electric potential of the return electrode and the electrosurgical tool are given as boundary conditions. Although the return electrode is fixed on the tissue, the electrosurgical tool is moved, and thus, the contact area changes interactively. The thermal phase determines the temperature distribution caused by Joule heating and temperature conduction. The governing equations of electric conduction and heat transfer are given by Laplace and heat equations.

$$\nabla^2 V = 0 \tag{1}$$

$$c\rho \frac{\partial T}{\partial t} = \lambda \nabla^2 T + \mathbf{J} \cdot \mathbf{E} \tag{2}$$

where V is voltage, T is absolute temperature, $\mathbf{J}$ is current density, $\mathbf{E}$ is electric field, and c, ρ, λ are specific heat, density, and thermal conductivity, respectively. Eq. 1 gives the electric potential distribution. Eq. 2 calculates the temperature distribution.

2.3 Structural phase

It is reported that material destruction in electrosurgery is caused from mechanical rupture [1]. The structural phase determines the structural change caused by vaporization and stress concentration. The stress is derived from the expansion of the volume caused by water vaporization. The volume expansion at the position $\mathbf{r}$ at the time t is given by

$$\triangle v(\mathbf{r},t) = \triangle v_{liq}(\mathbf{r},t) + \triangle v_{gas}(\mathbf{r},t) \tag{3}$$

where $\triangle v_{liq}(\mathbf{r},t), \triangle v_{gas}(\mathbf{r},t)$ are the expansion of water from the initial temperature and the expansion caused by the transition of water from liquid to vapor, respectively. This expansion leads deformation and the stress concentration. The equilibrium, strain-displacement relation, stress-strain relation, and constitutive equations are solved to calculate stress distribution. Finite Element Method(FEM) is used for the numerical solution. In the processes, Young modulus, Poisson's ratio, and breaking stress are considered. If the Mises stress is greater than the breaking stress, the elements in the area are removed to represent material destruction. The contact area between the tool and the tissue is updated from the moving direction of the tool, and the simulation is carried out repetitively by reconstructing the mechanical structure.

3 Interactive electrosurgical cutting simulation

3.1 Approach

This section describes a pre-processing method of electric potential. The approach is to reduce the computational cost in real-time processing by pre-processing independent of prior contact information. Fig. 3 shows the difference of the conventional and proposed methods. It can be assumed that the number of contact nodes is small, compared with the number of other nodes, i.e. non-contact nodes. Therefore, high-cost matrix operations of other nodes, such as the matrix inversion and factorization, require a large calculation time. The conventional method requires the contact information in the high-cost matrix operation, while the proposed method does not require the contact information in the high-cost matrix operation. Thus, the proposed method excludes the high-cost matrix operation from real-time processing to pre-processing.

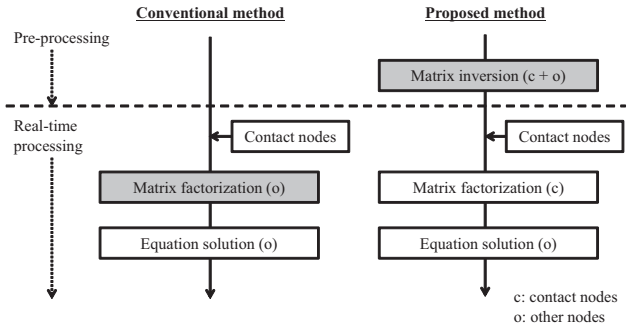

Figure 3: The difference of the conventional and proposed methods to solve a simultaneous equation for electric potential. The processes colored gray have high computational costs.

3.2 Conventional method: matrix factorization requiring prior contact information

In general, Laplace equation, as shown in Eq. 1, is solved by LU factorization, or similar matrix factorization methods. However, the contact nodes have to be known in advance. In other words, the change of contact nodes requires matrix factorization once again. Since the computational cost of matrix factorization is high, interactive manipulation that allows for the change of contact nodes becomes difficult.

First, the conventional method is described. After the contact nodes are given, the nodes are categorized into contact and other nodes, in order to solve Laplace equation,

$$\mathbf{K}\mathbf{u} = \mathbf{f} \tag{4}$$

$$\begin{pmatrix} \mathbf{K}_{oo} & \mathbf{K}_{oc} \\ \mathbf{K}_{co} & \mathbf{K}_{cc} \end{pmatrix} \begin{pmatrix} \mathbf{u}_o \\ \mathbf{u}_c \end{pmatrix} = \begin{pmatrix} \mathbf{f}_o \\ \mathbf{f}_c \end{pmatrix} \tag{5}$$

where $\mathbf{K}, \mathbf{u}, \mathbf{f}$ are the coefficient matrix, and the vectors of electric potential and electric density, respectively. The suffixes c, o represent the components of contact and other nodes, respectively. Here, $\mathbf{f}_o = \mathbf{0}$ gives:

$$\mathbf{K}_{oo}\mathbf{u}_o = -\mathbf{K}_{oc}\mathbf{u}_c \tag{6}$$

$$\mathbf{u}_o = -\mathbf{K}_{oo}^{-1}\mathbf{K}_{oc}\mathbf{u}_c \tag{7}$$

The order of Eq. 6 is the number of other nodes. As a result, the high computational cost of matrix factorization makes it difficult to achieve real-time simulation that allow for the interactive change of contact nodes.

3.3 Proposed method: matrix inversion independent of prior contact information

The proposed method inverts the whole coefficient matrix, before the contact nodes are given. This approach has the advantage of not requiring prior information regarding the contact nodes and thus reduces real-time computation through pre-processing time-consuming calculations. The process is as follows:

1. (Pre-processing): The inverse of coefficient matrix $\mathbf{L} = \mathbf{K}^{-1}$ is calculated, where $\mathbf{K}, \mathbf{u}, \mathbf{f}$ are the coefficient matrix and the vectors of electric potential and electric density, respectively.

$$\mathbf{K}\mathbf{u} = \mathbf{f} \tag{8}$$

$$\mathbf{u} = \mathbf{L}\mathbf{f} \tag{9}$$

2. (Real-time processing): Given the contact nodes between a tool and an object by interactive manipulation, $\mathbf{L}$ are arranged with the contact and other nodes. $\mathbf{f}_c$ is represented by a part of matrix L, $\mathbf{L}_{cc}$, where the suffixes c, o represent the components of contact and other nodes, respectively. Eq. 1 induces $\mathbf{f}_o = \mathbf{0}$.

$$\begin{pmatrix} \mathbf{u}_o \\ \mathbf{u}_c \end{pmatrix} = \begin{pmatrix} \mathbf{L}_{oo} & \mathbf{L}_{oc} \\ \mathbf{L}_{co} & \mathbf{L}_{cc} \end{pmatrix} \begin{pmatrix} \mathbf{f}_o \\ \mathbf{f}_c \end{pmatrix} \tag{10}$$

$$\mathbf{f}_c = \mathbf{L}_{cc}^{-1}\mathbf{u}_c \tag{11}$$

3. (Real-time processing): electric potential at non-contact nodes $\mathbf{u}_o$ is calculated.

$$\mathbf{u}_o = \mathbf{L}_{oc}\mathbf{f}_c \tag{12}$$

$$= \mathbf{L}_{oc}\mathbf{L}_{cc}^{-1}\mathbf{u}_c \tag{13}$$

Although the matrix inversion is computationally high, the order of Eq. 12 is only the number of contact nodes. Eq. 13 requires a low computation time because the matrix-vector multiplication is low cost. In summary, the first process in pre-processing is computationally high, and the second and third processes in real-time processing require low computational costs.

3.4 Process flow

The process flow of the proposed method is shown in Fig. 4. In real-time processing, the calculation of electrical-potential, temperature, and stress distribution are carried out after the collision between a virtual tool and a tissue model is detected. If a rupture is found in any element of the tissue model, the reconstruction process is launched. While the reconstruction is being processed in the back ground, the real-time processing is kept up. After the reconstruction, the time progress from the beginning of reconstruction to the end is re-calculated.

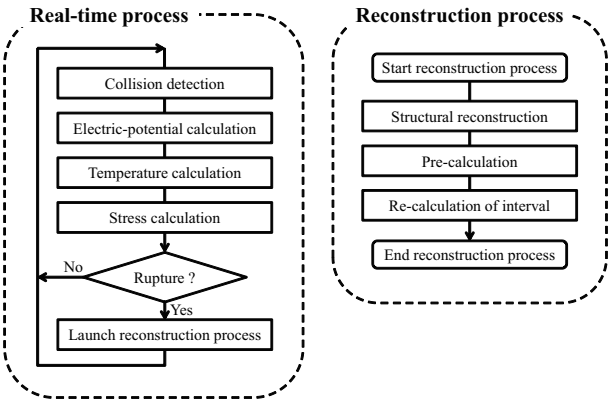

Figure 4: The process flow of electrosurgical cutting.

4 Experiments

4.1 Experimental setups

The simulation system was equipped with Intel CPU (Core i7 3.07GHz), 12GB main memory, and an nVidia GeForce GTX 580 graphics board. Intel Math Kernel Library was used for numerical solution including matrix operations. The object used in the simulation had 1013 nodes (tetrahedral mesh). The object size was 100 mm $\times$ 100 mm $\times$ 10 mm. Fig. 5 shows the shape of the object. Table 1 shows the applied physical parameters, which are derived from the studies using porcine liver [5, 9, 10]. The shape of the return electrode was a circle with a radius of 40 mm. In the simulation, the water evaporates at 100 °C, assuming that the effect of the stress on the vaporization is small enough to be ignored. The boundary conditions in the simulation are given in Table 2, where $\mathbf{n}$ is the normal vector, σ is the electric conductivity of the nodes, and λ is the heat conductivity.

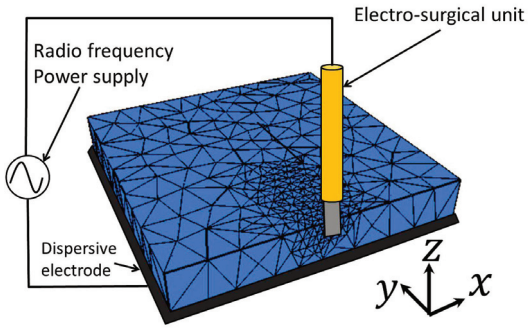

Figure 5: 3D object used in the simulation

Table 1: Main physical parameters in the simulation

Specific heat $\times$ density	$3.82 \times 10^6 \mathbf{J}/(^\circ C \cdot m^3)$
Heat conductivity	0.502 W/(m·° C)
Electric conductivity	0.144 S/m
Young modulus	4.75×10^4 Pa
Poisson's ratio	0.400
Critical stress	2.45×10^4 Pa

Table 2: Boundary conditions in the simulation

(a)Electrical phase

	Electric potential
Nodes contact with tool	V = 72 V
Nodes contact with return electrode	V = 0 V
Other boundary nodes	$\mathbf{n} \cdot (\sigma \nabla V) = 0$

(b)Thermal phase

	Temperature
Nodes contact with tool	$\mathbf{n} \cdot (\lambda \nabla T) = 0$
Nodes contact with return electrode	$\mathbf{n} \cdot (\lambda \nabla T) = 0$
Other boundary nodes	$\mathbf{n} \cdot (\lambda \nabla T) = 0$

4.2 Simulation results

Fig. 6 shows the simulation results of the calculation phases: (a) the distribution of the electric potential, (b) the distribution of the temperature, and (c) distribution of the stress. The electric potential around the contact nodes with the electrosurgical tool was high. The temperature of the nodes was increased by the Joule's heat, while the temperature was diffused in the object as time progressed. The stress increased after the vaporization of water in the elements. The elements whose stress was over the criteria were removed. The simulation was successfully continued during the reconstruction of the model. Fig. 7 shows the repetitive structure change by surgical cutting from the left side to the right side of the object.

Fig. 8 shows the interactive cutting simulation of electrosurgery. The objects used in the simulation had 643 and 1013 nodes, respectively. The contact nodes between the object and surgical tool were determined from the distance, and updated interactively. The surface was colored red, when the temperature was increased. The increased temperature is decreased gradually, because the heat diffusion is simulated based on Eq. 2.

4.3 Calculation time

Fig. 9 shows the calculation time of a series of the physics simulation. Fig. 9(a) is the calculation time of electric potential in the case of the proposed and conventional methods. The effect of parallelization of matrix operations was also examined. The result showed that the parallelization with three threads reduced 26.6% of the calculation time in the case of the conventional method. The result also showed that the proposed method reduced 45.1% of the calculation time, compared with the conventional method. The combination of the proposed method and parallelization reduced 59.7% of the calculation time in total. Fig. 9(b) shows the calculation time of each process and the total time. The result showed that the calculation time in the real-time processing was 30ms in the case of 506-noded object, so that the real-time simulation is achieved without a larger than 506-noded object. The pre-processing time was 114ms in the same simulation.

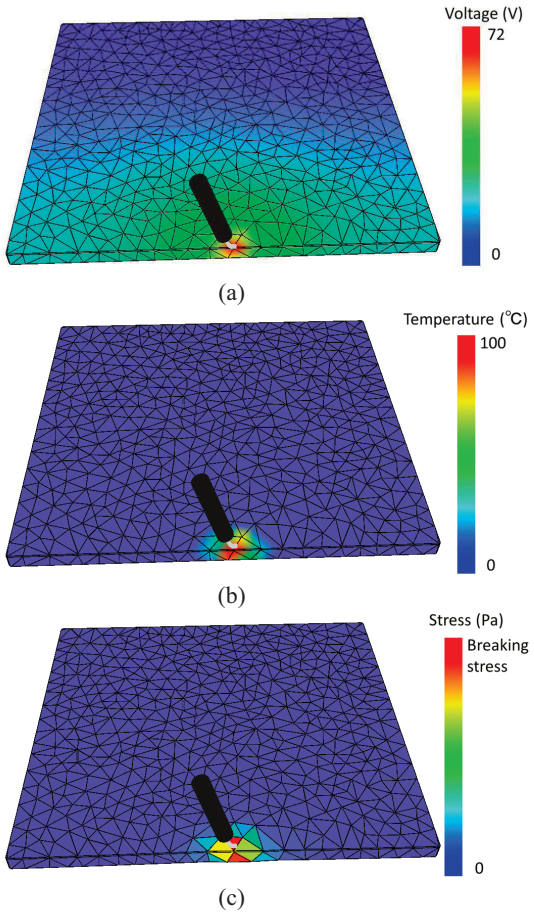

Figure 6: Simulation results: (a) the distribution of electric potential, (b) the distribution of temperature, and (c) the stress distribution

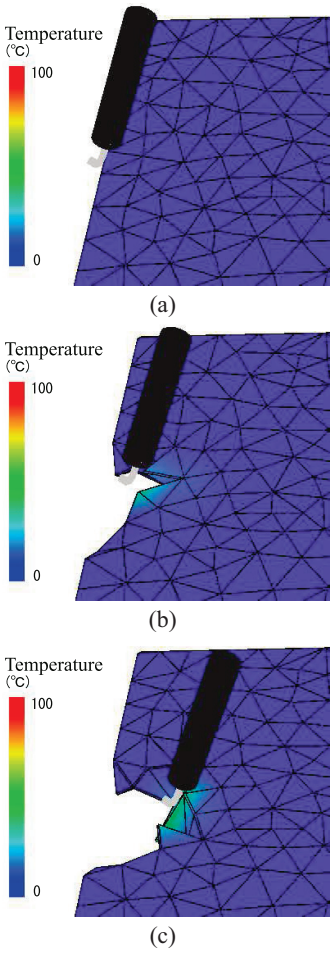

Figure 7: Simulation results of repetitive structure change in electrosurgical cutting

5 Conclusion

In this paper, we proposed an interactive simulation method of physics-based electrosurgical cutting. In particular, pre-processing, independent of contact information, reduced real-time calculations. The simulation results showed that the proposed method enabled an interactive simulation with consideration of a series of physical phases: electrical, thermal, and structural phases. In the clinical situation, it is occasional that the forces are applied on the object from the side. The simulation with the applied forces is a future work.

Acknowledgements

This study was partly supported by the Global COE Program "*in silico* medicine" at Osaka University.

References

[1] C. L. A. Ward and G. Collins. Material removal mechanisms in monopolar elecrosurgery. In *IEEE EMBC*, pages 1180–1183, 2007.

[2] E. J. Berjano. Theoretical modeling for radiofrequency ablation: state-of-the-art and challenges for the future. *Biomedical engineering online*, 5, 2006.

[3] C. Chen, M. Miga, and R. Galloway Jr. Optimizing electrode placement using finite element models in radiofrequency ablation treatment planning. *IEEE Trans Biomed Eng*, 2008.

[4] S. Cotin, H. Delingette, and N. Ayache. A hybrid elastic model allowing real-time cutting, deformations, and force feedback for surgery training and simulation. *The Visual Computer*, 16(7):437–452, 2000.

[5] C. Gabriel, S. Gabriel, and E. Corthout. The dielectric properties of biological tissues: I. literature survey. *Physics in Medicine and Biology*, 41(11):2231, 1996.

[6] G. Grinstein, D. Keim, and M. Ward. Laparoscopic electrosurgical complications. www.encision.com, October 2002.

[7] Y. Kuroda, S. Tanaka, M. Imura, and O. Oshiro. Electrical-thermal-structural coupling simulation for electrosurgery simulators. In *IEEE EMBC 2011*, 2011.

[8] A. Maciel and S. De. Physics-based real time laparoscopic electrosurgerysimulation. In *Medicine Meets Virtual Reality 16*, pages 272–274, 2008.

[9] S. H. Oh, B. I. Lee, E. J. Woo, S. Y. Lee, T.-S. Kim, O. Kwon, and J. K. Seo. Electrical conductivity images of biological tissue phantoms in mreit. *Physiological Measurement*, 26(2):S279, 2005.

[10] J. W. Valvano, J. R. Cochran, and K. R. Diller. Thermal conductivity and diffusivity of biomaterials measured with self-heated thermistors. *International Journal of Thermophysics*, 6:301–311, 1985. 10.1007/BF00522151.

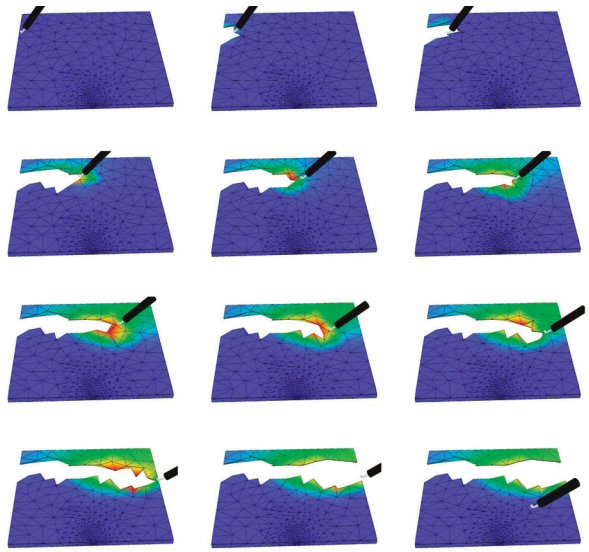

(a)

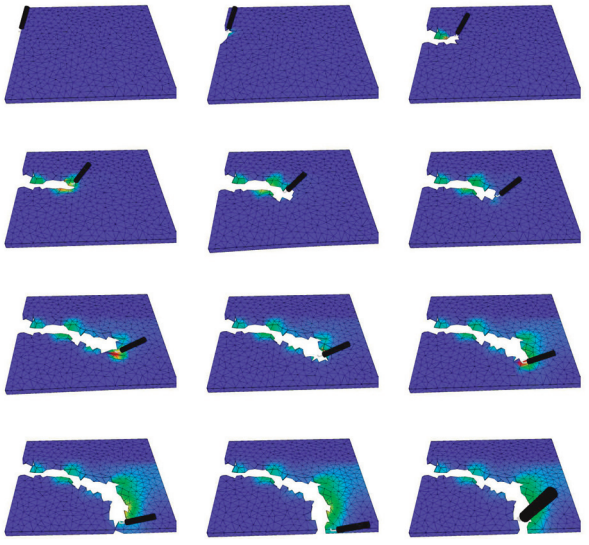

(b)

Figure 8: Interactive cutting simulation of electrosurgery: (a) 643 nodes (b) 1013 nodes

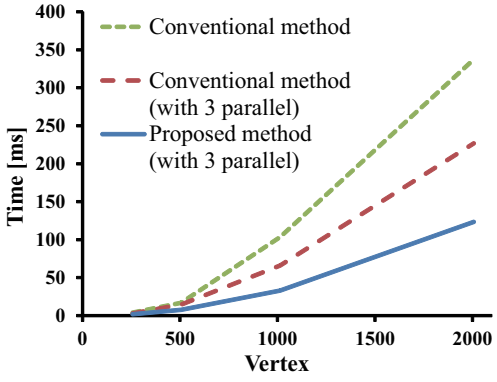

(a)

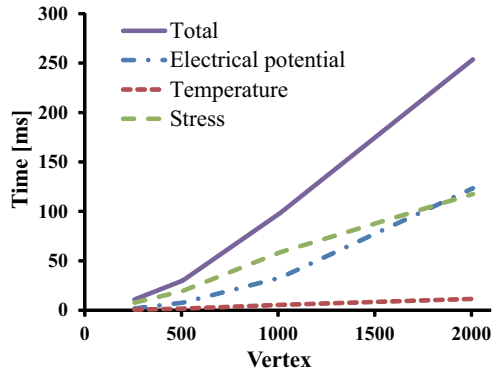

(b)

Figure 9: Calculation time of simulation: (a)electrical potential, (b)each procedure and whole procedures